Research Article

2348-8069

Ultrastructure of dorsal rim area of compound eyes of the male the red palm weevil, *Rhynchophorus ferrugineus* (Olivier) (Curculionidae: Rhynchophorinae): in relation to habitat

Nawal A. Al-Fuhaid*

Sattam Bin Abdul-Aziz University, College of Science and Humanities, Department of Biology, Kharj, Saudi Arabia

*Corresponding author: *nfheed@yahoo.com*

Abstract

The compound eyes of a male red palm weevil, *Rhynchophorus ferrugineus* (Olivier), were investigated using scanning techniques, specifically, the ommatidium in the dorsal rim area was studied by light and electron microscopy. Each eye contained 3000–3500 mostly hexagonal facets. No ocelli, corneal nipples or interommatidial hairs were found. The eye was of the acone and apposition types, with 8 retinular cells per ommatidium (two central, six peripherals).The peripheral distal and proximal rhabdome were composed of six separated rhabdomeres, with the separation between them increased by interretinular spaces. The central distal rhabdom consists ofr7, while the central proximal rhabdomeres was fused by R7 and R8. The microvilli of the peripheral distal rhabdomeres R2, R3, and, the central proximal R7, R8 were arranged in a three-dimensional pattern, where as distal R4 was warped around itself. The distal R7 and the proximal R1– R6 were possessed microvilli oriented in such away as to permit e-vector discrimination. The difference between the central and peripheral rhabdomeres in the two rhabdom regions. With regard to the microvillar arrangement implied the occurrence of the rhabdomeric twist. It was encountered only at the distal region, where the rhabdomeric organization displayed an effective strategy to improve absolute sensitivity, at the expense of the polarization of sensitivity, to overcome the particular problem of vision in dim habitats. A possible function in the perception of host related visual cues is proposed and discussed in relation to the plausible roles of the dorsal rim area in host location by male weevils.

Keywords: sexual dimorphism; facets; the polarization of light; rhabdomeric twist; vision cues

Introduction

Depending on the classification insect eyes, Exner (1891) distinguished the compound eyes apposition and superposition eyes. The organization of compound eyes plays an effective role the relationship between activity and phylogeny and aids the entomological to understand of species.

Lefroy (1906),Vidyasagar & Keshava-Bhat(1991), reported that the *Rhynchophorus ferrugineus* is one of the most economically disruptive stem-tissue-boring

pests of date palm. *Phoenix dactylifera* L., in many parts of the world. Aim of this study was to investigate the organization and ultrastructure of the dorsal rim area (DRA) of the compound eye the male red palm weevil, *Rhynchophorus ferrugineus* (Olivier) (Curculionidae: Rhynchophorinae), to determine its possible functional roles in the behavioral ecology of this pest, The DRA is of particular anatomical importance in insect vision (Labhart & Meyer 1999). The male eye was chosen for several reasons.

Aldryhim & Ayedh (2015) reported that the male *R. ferrugineus* showed a peak of three daily flight activities versus a peak of two for the female, suggesting that males initiate flight activity more readily than females. Likewise, Fanini et al. (2014) found that male red palm weevils were active earlier in the day than females in both native and invasive localities. But information about the male visual system in this family is vague and insufficient. For Rhynchophorinae , the only information comes from recent studies by Ili (2014) and Ili et al. (2016)which used transmission electron microscopy to study the compound eye of a red palm weevil of unidentified gender.

Materials and Methods

Ten males specimens of the red palm weevil, *Rhynchophorus ferrugineus*(Olivier), were obtained from Saudi Arabia, ranging from 3 to 3.8 cm in length and 1 to 1.5 cm in width. For electron and scanning microscopy techniques, followed by (Mishra & Meyer-Rochow 2008b) were fixed compound eyes at light adapted and during the day at around 12.00 PM. Their severed heads were split in half along the eye's sagittal plane, and the brain and air sacs were removed fixed for 1day in a cold mixture of 2% paraformaldehyde and 2.5%glutaraldehyde,and buffered in 0.1 mol/L cacodylate at a pH of 7.4. Following two washes in 0.1 mol/L cacodylate buffer, the specimens were then fixed for 1 h in 2% cacodylatebufferedOsO4. After three brief rinses in the same buffer and two in distilled water, the specimens were passed through a graded series of ethanol, before being immersed in acetone/Epon mixture (50:50) for 1 day.

Finally, the specimens were embedded in pure Epon resin and hardened for 3 days at a temperature of 60^0-C^0. Semi-thin and ultrathin sections were taken from a dorsal rim area of the dorsal eye. Semi-thin sections for light microscopy were cut on an ultra microtome(RMC Boeckeler)with a glass knife and stained with 0.5%aqueous solutions of toluidine blue on a hot plate for a few seconds. Ultrathin sections were cut with glass or diamond knives and supported on uncoated 300-mesh copper grids. The ultrathin sections were stained with Reynolds' lead citrate for 20 minutes and 2% aqueous uranyl acetate for 15minutes and finally observed under a Zeiss EM 10 transmission electron microscope, operated at 60 kV.

For observation by scanning electron microscopy (SEM), the eyes were removed from freshly-killed red palm weevils with a razor blade and affixed on adhesive tape. The eyes were then air-dried, coated with a thin layer of gold–palladium and viewed under a scanning electron microscope. On the SEM photo, a 1 mm^2 area of the eye was marked and all ommatidia inside this area were counted. The diameters of the facets (i.e., corner to corner distances of the hexagonal lenses)were determined from 15 randomly selected ommatidia. Photos of each eye were scanned into a computer to measure the eye surface areas with an imaging program(Image J). The total number of ommatidia per eye was extrapolated from the count of the 1 mm^{2}area. The error due to minor variations in the facet sizes and shapes was regarded as negligible.

Results

At dorsal lateral positions of the posterior edge occupy the two compound eyes of the male, *R. ferrugineus*, while the anterior edge of the eye runs parallel to the anterior wall of the rostrum (Fig. 1.A,B,C). The eyes are elongated to the extent that they meet each other. The two eyes are identical to each other on either side of the rostrum (Fig. 1.C). The separation between the dorsal sides of the left and right eyes is approximately 1mm (Fig. 1.A). The anterior–posterior axis measured ~ 0.6 mm and the dorsoventral axis ~ 2mm. SEM observation revealed that the total area of the dorsal and ventral region of the male compound eyes was less than that of the lateral region (Fig. 1.A, C).The eyes contain 3000–3800 ommatidia and are semicircular (Fig.1.A, D). Differences between the male and female rostrum of *R. ferrugineus* have been described by many researchers (for a review see: Esteban-Duran et al. 1998). but there is no evidence for sexual dimorphism with regard to the eyes.

The facets tend to flatness and more curved in the dorsal region and the inner distal area of the cornea is strongly convex (Figs. 1.B and2.A, B), smooth and without corneal nipples and hair in general of the eye area. The ommatidia are typically hexagonal (Fig. 1.D), with each facets spanning 20–35µm, at the dorsal region. The length and diameter ranges of the ommatidia are 200–270mm and20–35µm respectively so the diameter of the facets varies (20–35µm) (Fig. 2.A, B).

The cornea is laminated in appearance as external features the interfacial spaces are not clear but internally between each of the ommatidia it are clearly and deeply (Fig. 2.A, B, C).
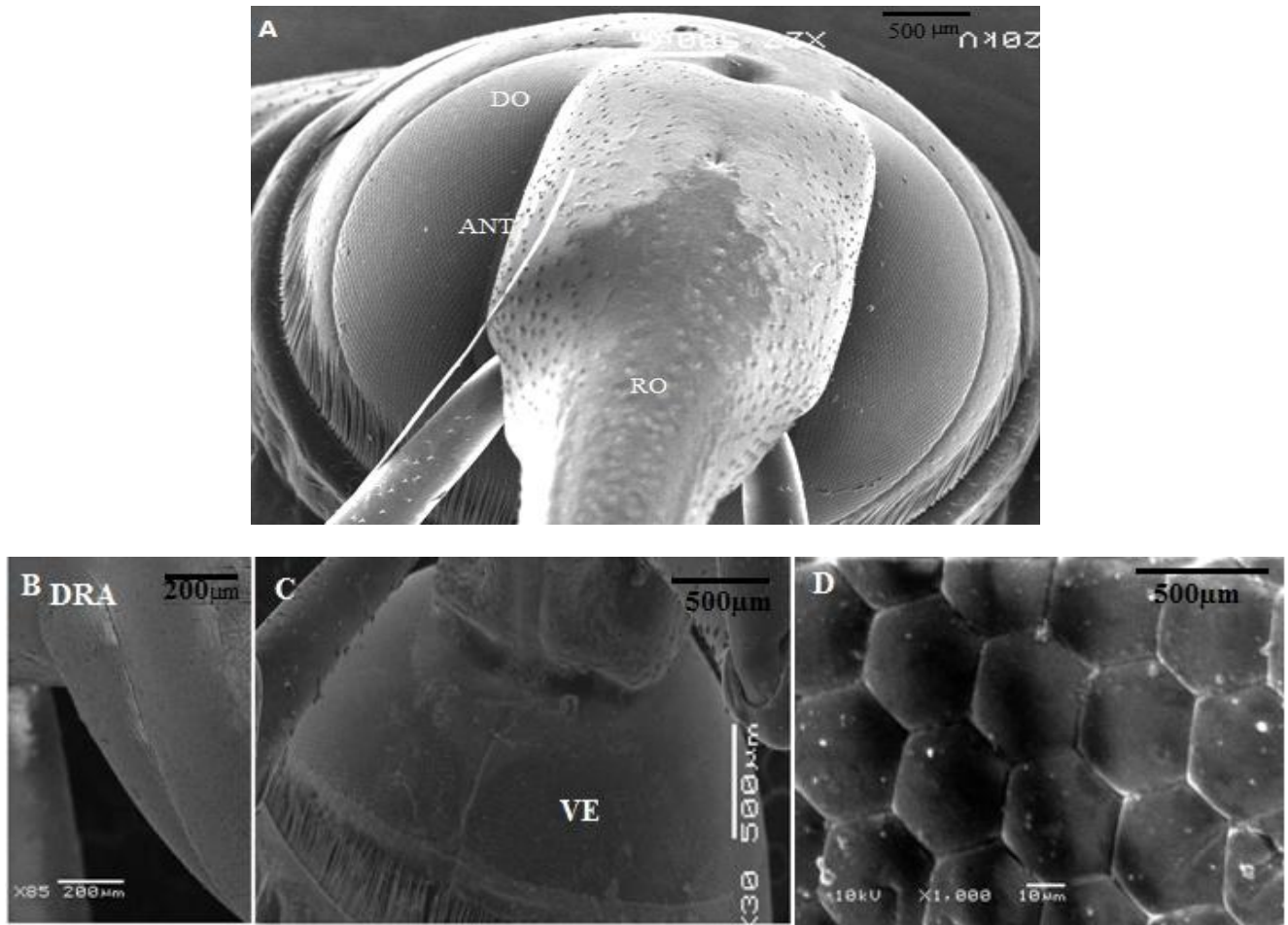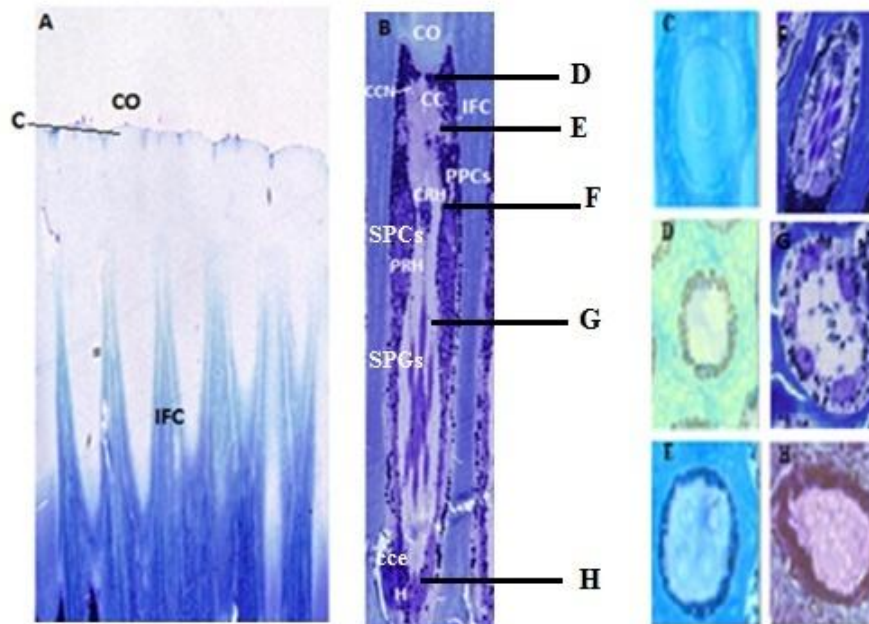
Fig. 1. Scanning electron micrographs of the compound eye male of *Rhynchophorous ferrugineus* (Olivier). **A**. head, showing laterally position of eyes on the head, being well separated by a prominent rostrum (RO), Each eye with facets well aligned in definitive rows and showing narrow the dorsal rim area (DRA) at top of the dorsal region (DO) and a some of the width of the anterior region(ANT) of the eyes. **B-D**. Top and lateral view of the dorsal region of the eye and the anterior-poster region. **E**. The ventral region (VE) both of the eyes being doggo beneath rostrum. **D**. Higher magnification of the hexagonal facets are smoothly.
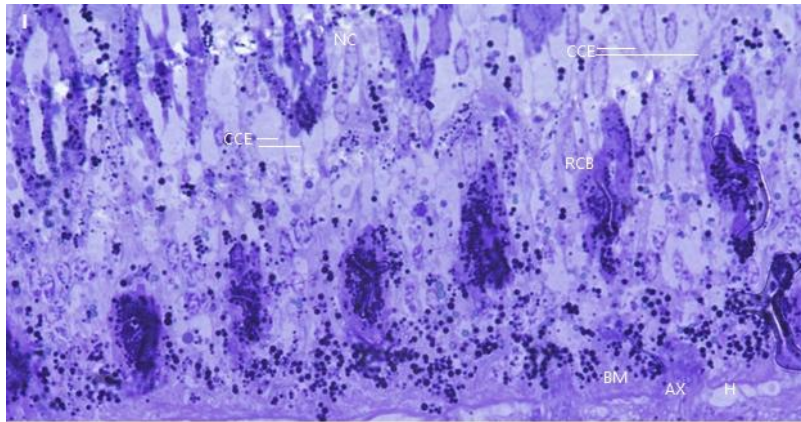
Fig. 2. Light micrographs of the ommatidia in the dorsal rim area of the eye male of *Rhynchophorous ferrugineus* (Olivier). **A, B**. Longitudinal perspective. **C-H.** Transverse sections showing the shortcuts on the right side of (**A-B**) by dark lines**.** cornea (C) and cone cells (CC) without any crystalline material, the latter being surrounded by two primary pigment cells (PPCs). Eight secondary pigment cells(SPCs) were surround every primary pigment. Obvious spacing between the central rhabdom (CRH) and the peripheral rhabdom (PRH) from distal until proximal rhabdom region of the retinula cell, this feature is including to light adapted. At proximal end appear some of retinula cell bodies(RCB) with nuclei, note the interfacetal corneal regions (IFC) between adjacent ommatidia. **B.** High magnification of the ommatidium showing the distal rhabdom (DRH) and the proximal rhabdom(PRH). Notable the radial pigment migration in the retinula cells which the primary and secondary pigments closely around the rhabdom (Rh) indicate to light adapted. **I**. Oblique section through the narrow cone cell extensions (CCE), white lines indicate to(CCE),which run far away at the basement membrane (BM) which run narrow with the axon bundles(AX), then penetrate (BM) by sporadic holes corresponding to the number the ommatidia and consisting of the eight retinula cells for each of them . Neuron nuclei (NC) it has spread between of the proximal retina. Heamacoel (H) was visible.

There are four cone cells per ommatidium which have a spherical shaped and nuclei up to 5µm in diameter cylindrical shaped, with convex distal face and strong concave proximal tip below the cornea (Fig. 2.B, E). Endoplasmic reticulum (ER) are around of the cone frontal single mitochondrion, multi-vesicular bodies, some membranes and granules also present (Fig. 3.A). The cone cells make a tract then splits and forms the inter-cellular space between the cells of the retina to its end (Fig. 3.B).

The four cone cells at each ommatidium were enclosed by the two primary pigment cells (PPCs). The cytoplasm was abundant mitochondria and pigment grains (PGs), both of them have electron density cytoplasm, with diameter from 0.6 to 0.9µm and 0.4 to 0.8µm respectively. The secondary pigment granules(SPGs) belonged to the secondary pigment cells which proximately in 8~10 µm and have a low electron density with the diameter in 0.6µm (Fig. 2.B-F and 3.A, B). the PGs are aid the eye to dark/light adaption, by migration at just peripheral between distal and proximity of the retinal cells, if the migration start to distal rhabdom that indicates to light adapted (Fig. 2.B) is showed the light adapted of the

eye. Furthermore, at end of that the region, a smaller size gray pigments are wide spread.

A. RETINULA CELLS AND RHABDOM

A.1.Distal Retinula Cells

For numbering of rhabdomeres. Followed the system used by Wachmann(1977) to number the retinula cells. The ommatidia at dorsal rim area possess the open rhabdom system, the diameter of the distal rhabdom was 25µm, are consisting of six peripheral ring of retinal cells which have R1– R6 and surrounded and separated from the seventh central retinal cell with R7 at distal region while eight retinal cell is not present. R7 resembles a fin hand or escalope shell and have microvilli arranged in one direction (Fig. 3.B, C). Also, the R1–R6 are separated from together, because of interretinal spaces (IRSs) between them, (Fig. 3.C, F) showing the R7 microvilli run parallel with those of the R2 and R3 and perpendicular to those ofR1, R5 and R6 while completely traversing the R4 microvilli, generally the microvilli of the R1–R6 form a mirror image of each other's (Fig. 3.C, D).
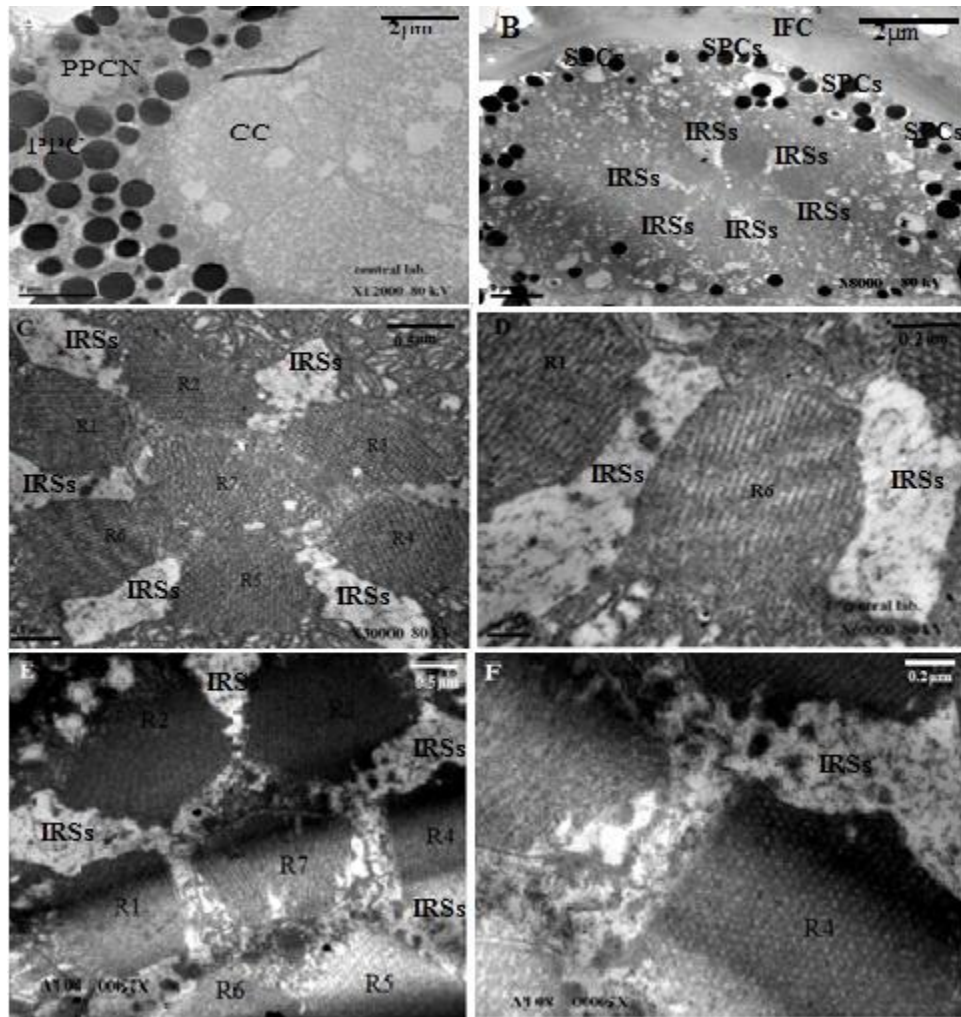
Fig. 3. Transmission electron micrographs through the distal region of the dorsal rim area of the eye male of *Rhynchophorous ferrugineus* (Olivier). **A**. the four cone cells, nuclei and some of the primary pigment cells (PPCs) appears nuclei one of the primary pigment cells (PPCN) at edge of the left the cone cell (CC). **B-F**. The open rhabdom and interretinal space (IRS) are clearly, the secondary pigment cells(SPCs) and secondary pigment granules (SPGs), there abundant (MT). Note the empty areas from organelles developed in the interfacetal corneal regions (IFC). **C**. the one centrally retina cell it is seventh, R7. **D**. Higher magnification showing a parallel orientation of the microvilli of R1 and R6 and (IRSs). **E**. Rhabdom of another ommatidia in same the level . Note the R2 microvilli have two orientations oblique orientation of the microvilli of R4 (wavy arrow) indicate to cytoplasm extensions which emanate from peripheral rhabdomeres border, (arrows head) indicate to the desmosomes between neighboring retinula cells. **F**. Higher magnification of the cytoplasm extensions between the peripheral and central system rhabdom, note R4 microvilli arrangement in oblique directions and exhibit a tubular nature, also, cytoplasm extensions (wavy arrows) between the peripheral and central system rhabdom.

The interfacetal corneal (IFC) regions are notably between neighboring ommatidia. A few micrometers further into the eye, the diameter is 23µm. The R7 exhibit an incoherent appearance especially at the center and we can identify the border of the seventh and eighth retinula cells (Fig. 4.B, C).

Moreover, the microvilli of R1– R6 in three directions. Generally, the edges of the peripheral and central rhabdomeres are disconnected resembling budding off of some membranes wrapped are commonly found in the cytoplasm close to the microvillar bases. (Fig. 4.B). The presence of numerous cytoplasm content at this level is noteworthy (Fig. 4.A, D).
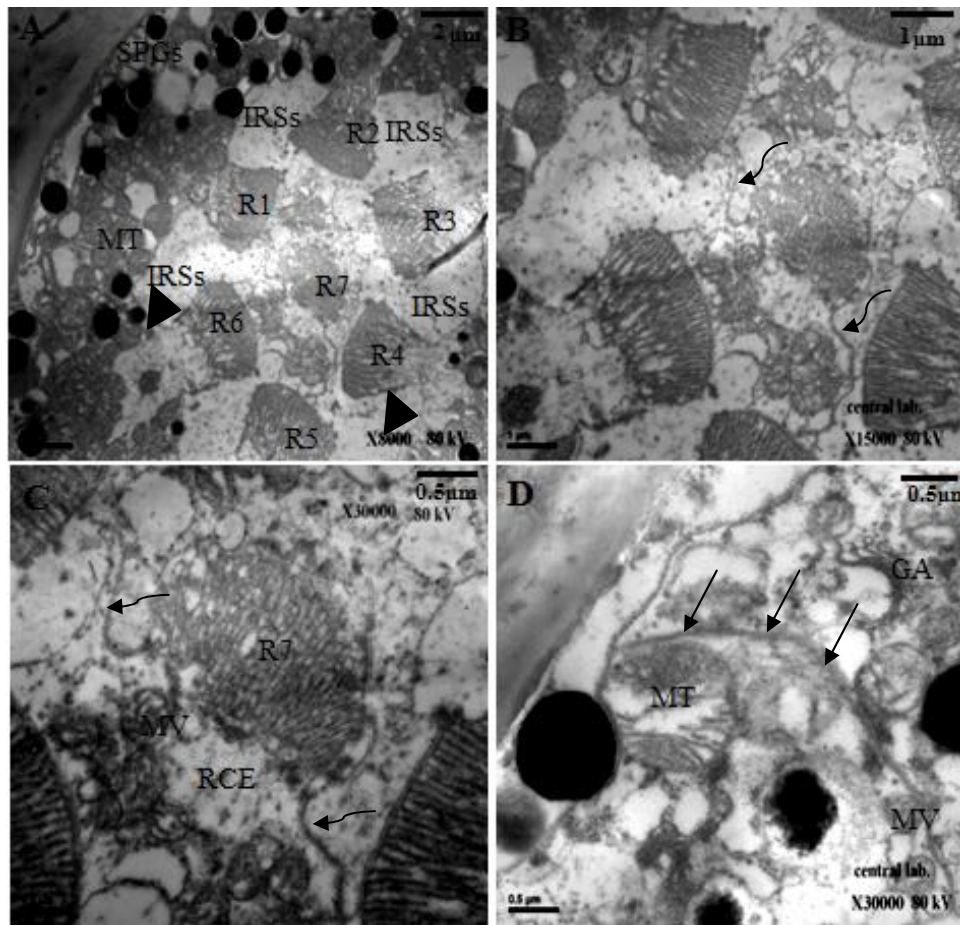
Fig. 4. Transverse sections through the end of the distal region of one ommatidia in the dorsal rim area. **A–C**. Showing appear a disconnected at R7 apex particularly, wavy arrows indicate to the cytoplasm extensions between the peripheral and central system of rhabdomeres. Note the retinula cell eight (RCE) without rhabdom, and increased area of the tow central cell and more of (MT) (arrows head) indicate to the desmosomes. **D**. Long arrows are indicate to cone cell tract which pass through the numerous of the secondary pigment cells (SPCs), the secondary pigment granules (SPGs), mitochondria(MT), multi-vesicular (MV) and Golgi apparatus(GA).

A. 2. Proximal Retinula Cells

Proximally, the diameter is 22µm, R8 appears fused with R7, and have microvilli are tightly and clearly aligned with a flower shape. The microvilli arranged in the R7, R8 are in three direction versus those in same direction at R1– R6. The microvilli of the R8 run in the same direction as those of R2, R3, R5 and R6and those of R7 perpendicular to each other (Fig. 5.B, C). interestingly, the development of the IRSs becomes bubble like and an IFC region is present (Fig. 5.A, B). Even more proximally, the separation of the line adhesion between R7 and R8 is clear.

Deeper at the end of the proximal region, clearly disconnected from the R7 and R8, while the R1–R6 has an irregular appearance for two reasons. First, the IRSs are widened and nested with each other. Second, all of the R1–R6 are diminished in size. The ommatidia become closer without overlapping owing to the compression of the IFC areas (Fig. 6). Every bundle composed of eight retinal axons which involved around one central fiber (Fig. 7.C, D). There is a glial cell, fibers and pigment granular (Fig. 7.A-D), but not tapetum of tracheoles above or below the basement is developed, the extensions of the cone cells are round up at the basement membrane (Fig. 2.H, I and 7.C, D). At the end of the proximal region, some unidentified intercellular structures are visible and the nuclei have a pellet shape, the cell walls are at the thickest and the cytoplasm is not empty but strewn with small particles (Fig. 7.B).
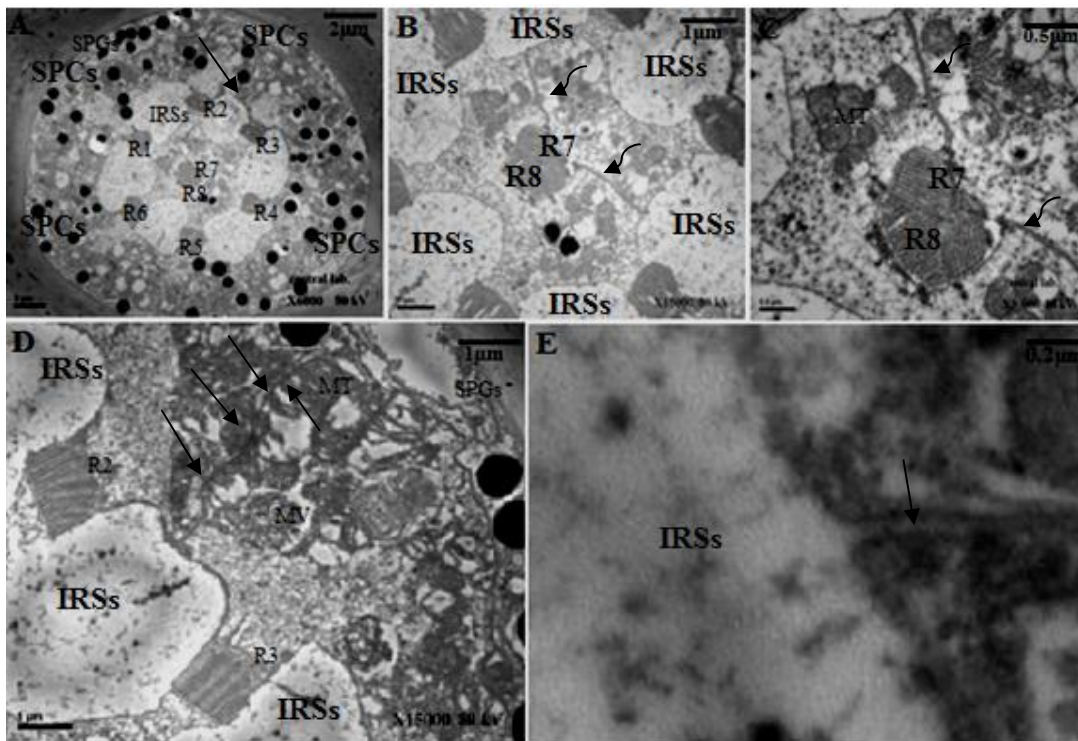
Fig. 5. Transverse sections through the start of the proximal region of one ommatidia in the dorsal rim area. **A**. Visible cone cell tract eight around the retina cell are penetrate between the pigment granular. Long arrows indicate to cone cell tract. **B–E**. Higher magnification of the peripheral and central system. **B– C**. Occurrence R8 was fusion with R7 and the R7 microvilli arrange in several directions, but R8 was not sent a cytoplasm extensions like R7, all rhabdomeres are smaller than interretinal space (IRSs), (wavy arrows) indicate to cytoplasm extensions but with new connect with two of the interretinal space (IRSs). **D**. Note connected the cone cell tract with interretinal space (IRSs). **E**. the enlargement the end of the cone tract at this point reveal the unquestionably the origin of the interretinal space(IRSs).
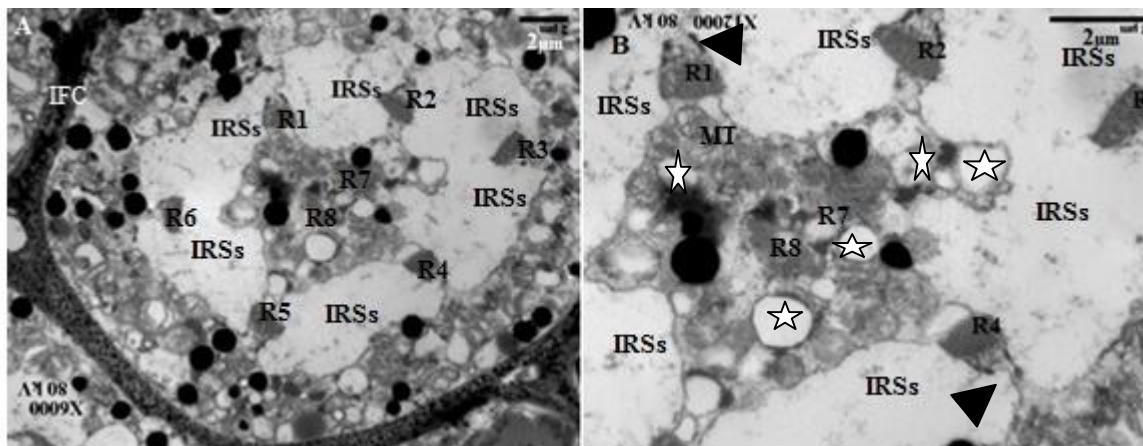

Fig. 6. Transverse sections through the end of the proximal region. **A.** Visible the decreased of the interfacetal corneal regions(IFC), all rhabdomeres are scrappy appearance and smaller than interretinal space (IRSs), notable the change of the occupy position of the R2 and R3. **B.** Higher magnification revealed the contributions of the most of the interretinal spaces(IRSs). Disintegration of the R7 and R8 and the shrink the peripheral rhabdomeres. the cytoplasm of the retinual cells content some vascular with foam shape (white star) indicate to the vascular foam, pigment granule, mitochondria (MT) and multi-vesicular (MV), arrows head indicate to the desmosomes.
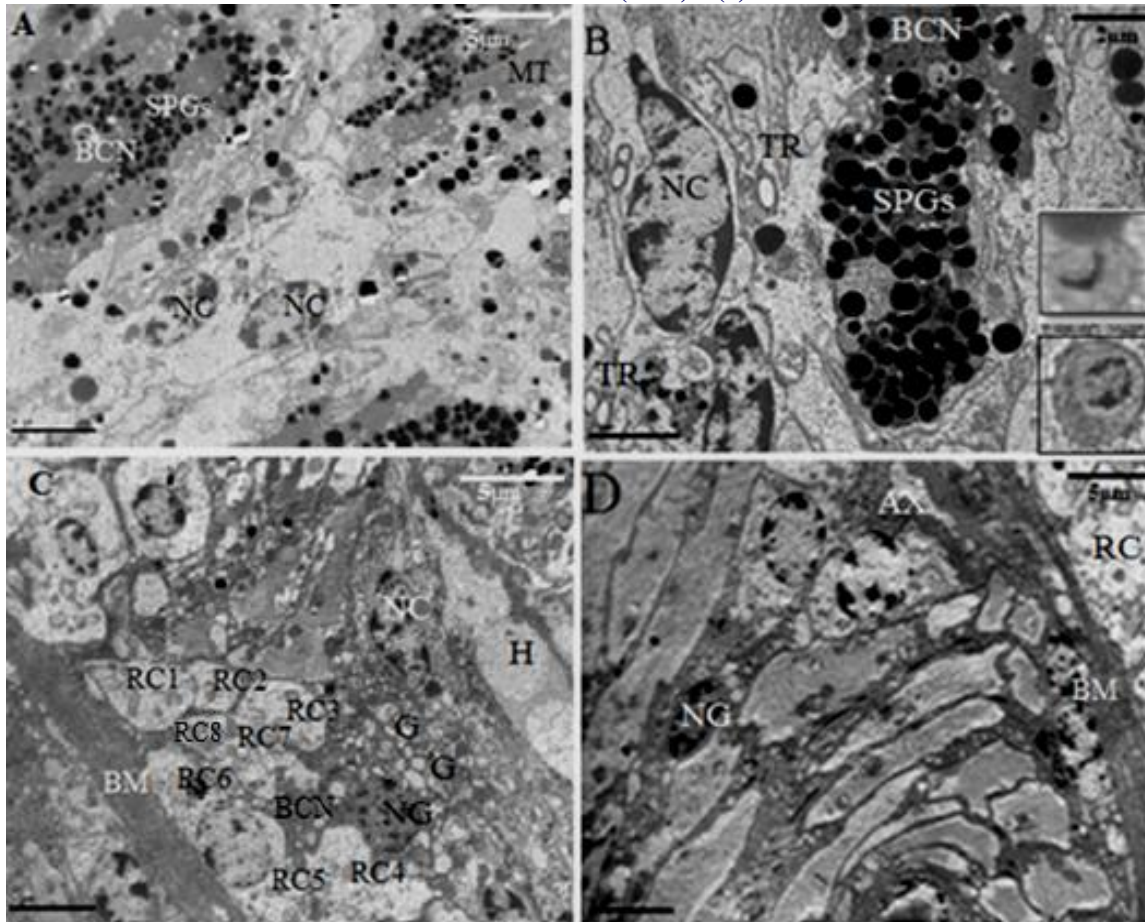
Fig.7. Transmission electron micrographs of the slightly oblique section through the most proximal region of retina the dorsal rim area the eye male of *Rhynchophorous ferrugineus* (Olivier). **A**. At this level, the rhabdomeres of the central and peripheral retinal cells are disappear, and has sufficient space to accommodate a variety of organelles, most notably pigment grains, mitochondria (MT), the basal retinula (BCN).The secondary pigment grains(SPGs). **B**. Higher magnification of the basal retinula cell (BCN) which cytoplasm was crowded by pigment grains and mitochondria, neuron nuclei(NC) and little of the tracheoles (TR) are spread between the ommatidium. The inset is higher magnification the unknown the intercellular structure.
C. Nearly of the basement membrane (BM) the eight retinal cells are turned into axons(AX) and surrounding the basal retinula cell (BCN) with their nuclei, also the cytoplasm containing of the mitochondria and neurotubules. The cytoplasm have less dense, pigment granules are absent here. The glia are inter with and around of the axon. Nucleus of the glia (NG), haemocoel(H) are visible. **D**. One of many sporadic holes in the basement membranes (BM) showing one axon bundle(AX) are passed through it, note a neurotubules and neurofilamentes are present in axon cytoplasm, residual body and muscle fibers are around the axon bundle after pass the basement membrane. Heamacoel (H) visible also.

Discussion

Depending on the classification system of the retina cells (Wachmann 1979) reported the Grundmuster1 was properties on the open rhabdom in this study. SEM observations revealed that the facets size of the dorsal rim area assumed that wide facets sizes were related to their functional importance correlated with the amount of light received by each facet at this region.

Somanathan et al. (2009) and Warrant (1999) previously reported the correlation between polarization vision, behavior and time of day, so that interpreted the diurnal relatives and polarization vision may play an important role in the long-distance homing flights of the diurnal-crepuscular male of *R. ferrugineus*. Dark/light adaption is also presumably because after the pupation and larval stages they spend long periods inside the palm trunk, where they complete their remaining life cycle, some of the males started has been emerging from of the palm trunk.

That is, they must emerge from the dark, humid and high- temperature ecology of the palm trunk then search for a new host and return to the conditions of the palm trunk. It is thus to be expected that the males will possess compound eyes with structures capable and deservedly of the dark/ light adaption, including sensitivity to the polarization of light in crepuscular or daylight hours.

the frontal position of the eyes and their curved surfaces with some flat areas and the corneal facets lenses, possibly this feature provide the main focusing power. This supportably features for DRA to exposure for a longer period of sunlight. According to (Meyer-Rochow& Horridge 1975), thick corneas are typical of many coleopteran, also typical of diurnal insects, like this weevils. Generally, the thick cornea protects the eye of the male *R. ferrugineus* while drilling in wood the palm trunk.

The cornea is elongated between the facets of the ommatidia which arrive the nuclear region before the basic membrane. It may be that elongation provides physical support and increases in the convergence of the inclined ommatidia with each other by convoluting the eyes around the rostrum, then offsetting together underneath the rostrum. Also, the rostrum protects the head and compound eye from damage caused by stray palm tissue while the male *R. ferrugineus* is boring into it, as well as while walking and flying.

There is no crystalline cone, (Grenacher 1879) consideration an ommatidium of this type is considered "acone" the eye has a strongly convex inner surface. These feature is typical of many nocturnal insects which provide further indirect evidence that the male *R. ferrugineus* is a cave insect or one habitually deprived of light.

The light adaption of the studied eyes, which fixed already at light adapted, displayed by closely of primary and secondary pigment granules around the ommatidial aperture far away from almost the proximal rhabdom to distal rhabdom, also, with narrowing of cone cells(Fig. 2.B). (Nilsson 1989;Nordstrom & Warrant 2000) mention that the typical aspects of light adapted. Non-Proliferation of the SPCs at all levels of the rhabdom inter retinula cells. This interpreted to imply an only distribution of the absorbed light along the interior axis because of the location of the cells far from the edges of the peripheral rhabdomeres as well as their absence around the central rhabdomere, also, that situation are suggesting a role in lateral absorption.

Several researchers like (Burakova & Mazokhin-Porshnyakov 1982; Mishra & Meyer-Rochow 2008a) confirmed that the vesicles originate from inflation of the interretinular strands and are simply extensions of the cone cells. Shaw (1978) considered the presence of vesicles around the rhabdomere to be a typical feature of dark/light adaption. The location of the Interretinular Spaces IRSs suggests two possible functions.

The first is to make physical contact with the rhabdomeres because both of them disappear in the nuclear region. The second, physiological function by increase sensitivity at the cost of resolution the presence of a palisade, which bodice the pigment granules away from the rhabdom. Finally, accordingly to (Horridge& Barnard 1965) this IRSs have a light-guiding function apparently to protect the photoreceptors from damage by the allowing of stray light to entire the eyes.

A. RETINULA CELLS AND RHABDOM

A.1.Distal Retinula Cells

The rhabdom is long and wide at the distal start and becomes very narrow at the most proximal end. (Horridge& Barnard 1965; Land 1981; Stavenga 2003) reported that the long rhabdom allows the receptor to collect more light and increasing the sensitivity, this feature is common in nocturnal and crepuscular insects. Although the eye examined here exhibits light adaption, there is strong evidence that this eye has an anatomical design optimized for vision in dim light.

According to(Eguchi 1999; Horváth & Varju 2004; Laughlin et al. 1975; Snyder1973) there is a relationship between the directions of the microvilli in the rhabdomeres and certain physiological functions, such as resolution and absolute sensitivity which depend on how the photoreceptors receive the light, moreover the arrangement of the microvilli facilitates e-vector detection because parallel microvilli with small diameters not only seem to display the highest polarization sensitivity and most sensitive to the UV part of the spectrum, the R1–R6 and R7 respectively have the microvilli with the smallest diameters, that the arrangement suggested that the absolute sensitivity higher at R1–R6 while the polarization sensitivity with in R1–R6 is believed to become destructive due to neural superposition .i.e., the summation of information from rhabdomeres with microvilli aligned in different orientations (Kirschfeld& Snyder1975).

The R7 was composed of microvilli aligned in the same direction and narrow. These aspects presumably aid the detection of the e-vector of polarized light. According to (Lin1993) the microvilli aligned in the same direction is distinguished to the green receptors and the polarization sensitivity is highest because it able to detected the e-vector. (Kirschfeld1969; Laughlin et al. 1975) reported that the polarized light is maximally absorbed when the microvilliis parallel to the axis of e-vector of polarized light. Also, According to(Monalisa& Benno 2006) that appropriate to the position the distal R7 microvilli because it is likely to be in confrontation permanent during daytime.

The second distal rhabdomeres give a contrasting appearance in several respects, whereby(Chamberlain et al. 1986; Meyer-Rochow&Tiang1984)with respect to the presence of membrane whorls and vesicular material the rhabdom edge appears to be consistent with the phenomenon of light-induced photoreceptor damage. The increased mitochondrial numbers and the morphological changes in the appearance of R7 are noteworthy. The system probably has a high energy requirement, which may be related to the fusing of the eighth rhabdom R8 with the seventh rhabdom R7.

End the distal rhabdom shows a strong indication of rhabdomeric twist, but not twisted uniformly along their entire length and that there was no contrast in the rates of twist in the different ommatidia . However, there was twist angles in the opposite twisting directions,(Altner& Burkhardt1981; Smola&Tscharntke1979) mention thus causing a reduction of the polarization sensitivity, preventing screening and especially effective in absorbing unpolarized light

A. 2. Proximal Retinula Cells

The arrangement and possible functions of the R1– R6 microvilli are may be similar to that of the level above but arranged more closely and smaller in size. In particular, R7acts as a polarization filter enhancing the polarization sensitivity ofR8. Snyder(1973) description the effect of placing one rhabdomere on top of another is to increase the polarization sensitivity of the lower rhabdomere, the longer the top rhabdomere the greater the effect. Stark et al.(1976) assumed the yellow-green receptor of Dipterans has been shown to correspond to R8, while according to (Bennett1978) its spectral sensitivity is strongly affected by its position below R7 in the *Scolytid* ommatidium.

Indeed the IRSs between with the tiny proximal rhabdomeres along most of the rhabdom s length allow it is to scatter a broader spectrum of light than is actually absorbed, a situation that is useful for diurnal insects, like this male weevil. Labhart & Meyer (1999) suggested that the structure like the IRSs are increased the absolute sensitivity. The basement membrane is characterized by the absence of tapetum of tracheoles and pigment granules. There are several scattered indications that the male *R. ferrugineus* is adapted to live at low concentrations of O2 in the palm trunk, like other species of insects with cryptic habitats.

Functional and Behavioral Considerations

Based on the anatomy of the dorsal rim of the compound eyes of the male red palm weevil, *Rhynchophorus ferrugineus* shows evidence of possessing the integrated functioning of at least two visual subsystems: a green-sensitive motion-detecting system at the central distal rhabdom and peripheral proximal rhabdom, and a UV-sensitive navigational system at the peripheral distal rhabdom and central proximal rhabdom. The required sophistication is evident in the design of the retina, which conforms to a mixture of the photopic and scotopic types at all levels along the length of the rhabdom to ensure a balance between resolution and sensitivity If some of the males which get out from the palm tree it meaning they are lives indeed two-thirds of its life cycle is spent in the dark making it relatively starved of light. Nonetheless, the male *R. ferrugineus* suffers no loss of vision during trips or when laboratory reared, also have particular visual abilities. These adaptations may be among the reasons for the wide spread of this insect. While the olfactory sense of the male *R. ferrugineus*is certainly the most important in determining its orientation toward the date palm tree, the importance of vision,should not be neglected. In flying toward these olfactory stimuli, the male *R. ferrugineus* must be able to avoid colliding with other trees, by locating an open and brightly it space to travel through until to reaching a palm-shaded environment.

Consequently, it is recommended that newly planted palms be spaced at distances that reduce shade, which provides a high density of short wavelengths. This reduction in the shade would thereby reduce the spread of the male *R. ferrugineus*. As for the palm groves, it is appropriate to control the entry and exit of the male *R. ferrugineus* from these by the thoughtful distribution of sources of bright light or light traps in

conjunction with the peak of the flight activity, especially at dawn and dusk.

Phylogenetic Considerations

Taxonomically, we have limited information and data about the compound eyes of (Arnett1968; Agee & Elder1970; Gordon &Winfree1978; Wachmann1979; Caveney1986; Mora2014). Wachmann (1979) concluded that the most archaic and perhaps original rhabdom type still occurs in most Curculionids, not only in Rhynchophorinae (Ili 2014). All of the above reported about apposition acone-type eyes for Curculionidae . The rhabdomeric twist is found not only in the eye of the male *R. ferrugineus* but in all Curculionids.

Acknowledgments

References

Agee HR, Elder HW. 1970. Histology of the compound eye of the boll weevil. Annals of the Entomological Society of America 63: 1654–1656.

Aldryhim YN, Ayedh HYA. 2015. Diel flight activity patterns of the red palm weevil (Coleoptera: Curculionidae) as monitored by smart traps. Florida Entomologist 98: 1019–1024.

Altner I, Burkhardt D. 1981. Fine structure of the ommatidia and the occurrence of rhabdomeric twist in the dorsal eye of male *Bibio marci* (Diptera, Nematocera, Bibionidae). Cell and Tissue Research 215: 607–623.

Arnett RH. 1968. The Beetles of the United States: A Manual for Identification. American Entomological Institute, Ann Arbor, MI.

Bennett LJ. 1978. The Spectral Response of Scolytids (Coleoptera: Scolytidae) to Visible Light: A Morphological, Behavioral and Electrophysiological Study. Theses,Simon Fraser University, Dept. of Biological Sciences.

Burakova O, Mazokhin-Porshnyakov G. 1982. Electron microscopy of the compound eye in *Haematopota pluvialis L.*(Diptera, Tabanidae). Entomological Review 61: 26–33.

Caveney S. 1986. The phylogenetic significance of ommatidium structure in the compound eyes of polyphagan beetles. Canadian Journal of Zoology 64: 1787–1819.

Chamberlain SC, Meyer-Rochow VB, Dossert WP. 1986. Morphology of the compound eye of the giant deep-sea isopod *Bathynomus giganteus*. Journal of Morphology 189: 145–156.

Eguchi E. 1999. Polarized light vision and rhabdom, pp. 33–46 *In* Eguchi E, Tominaga Y [eds.], Atlas of Arthropod Sensory Receptors: Dynamic Morphology in Relation to Function. Springer, Berlin, Heidelberg.

Esteban-Duran J, Yela J, Crespo FB, Alvarez AJ. 1998. Biology of redpalm weevil *Rhynchophorus ferrugineus* (Olivier) in laboratory and field: cycle in captivity, biological characteristics in its introduction zone in Spain and biological detection methods and possible control (Coleoptera: Curculionidae: Rhynchophorinae). Boletin de Sanidad Vegetal. Plagas 24: 737–748.

Exner S. 1891. Die Physiologie der Facettirten Augen von Krebsen und Insecten: Eine Studie. Franz Deuticke, Leipzig-Wien.

Fanini L, Longo S, Cervo R, Roversi PF, Mazza G. 2014. Daily activity and non-random occurrence of captures in the Asian palm weevils. Ethology Ecology & Evolution 26: 195–203.

Gordon H, Winfree AT. 1978. A single spiral artefact in arthropod cuticle. Tissue and Cell 10: 39–50.

Grenacher H. 1879. Untersuchungen Über das Sehorgan der Arthropoden: Insbesondere der Spinnen, Insecten und Crustaceen. Verlag von Vandenhoeck und Ruprecht, Göttingen.

Horridge GA, Barnard PBT. 1965. Movement of palisade in locust retinula cells when illuminated. Quarterly Journal of Microscopical Science 106: 131–136.

Horváth G, Varju D, 2004. Polarized Light in Animal Vision: Polarization Patterns in Nature.Springer, Berlin, Heidelberg.

Ili M. 2014. Funkcionalne in Anatomske Zna ilnosti Mrežnice Palmovega Ril karja (*Rhynchophorus ferrugineus*). Univerza v LjubljaniBiotehniška Fakulteta, Magistrsko Delo.

Ilic M, Pirih P, Belusic G. 2016. Four photoreceptor classes in the open rhabdom eye of the red palm weevil, *Rynchophorus ferrugineus*Olivier. Journal of Comparative Physiology A 202: 203–213.

Kirschfeld K. 1969. Absorption properties of photopigments in single rods, cones and rhabdomeres, pp. 116–136 *In* Reichardt W [ed.], Processing of Optical Data by Organisms and by Machines. Academic Press, New York.

Kirschfeld K, Snyder AW. 1975. Waveguide mode effects, birefringence and dichroism in fly photoreceptors, pp. 56–77 *In* Snyder AW, Menzel R [eds.], Photoreceptor Optics. Springer, Berlin.

Labhart T, Meyer EP. 1999. Detectors for polarized skylight in insects: a survey of ommatidial specializations in the dorsal rim area of the compound eye. Microscopy Research and Technique 47: 368–379.

Land MF. 1981. Optics and vision in invertebrates, pp. 471–592 *In* Autrum H [ed.], Handbook of Sensory Physiology. Springer-Verlag, Berlin.

Laughlin SB, Menzel R, Snyder AW. 1975. Membranes, dichroism and receptor sensitivity, pp. 237–259 *In* Snyder AW, Menzel R [eds.], Photoreceptor Optics. Springer, Berlin.

Lefroy H. 1906. The More Important Insects Injurious to Indian Agriculture. Government Press, Calcutta, India.

Lin JT. 1993. Identification of photoreceptor locations in the compound eye of *Coccinella septempunctata* Linnaeus (Coleoptera, Coccinellidae). Journal of Insect Physiology 39: 555–562.

Meyer-Rochow VB, Horridge GA. 1975. The eye of *Anoplognathus* (Coleoptera, Scarabaeidae). Proceedings of the Royal Society of London. Series B. Biological Sciences 188: 1–30.

Meyer-Rochow VB, Tiang KM. 1984. The eye of *Jasus edwardsii* (Crustacea, Decapoda, Palinuridae): electrophysiology, histology, and behavior. Zoologica 45: 1–68.

Mishra M, Meyer-Rochow VB. 2008a. Eyes of male and female *Orgyia antiqua* (Lepidoptera; Lymantriidae) react differently to an exposure with UV-A. Micron 39: 471–480.

Mishra M. Meyer-Rochow VB. 2008b. Fine structural description of the compound eye of the madagascar 'hissing cockroach' *Gromphadorhina portentosa* (Dictyoptera: Blaberidae). Insect Science 15: 179–192.

Monalisa M, Benno MRV. 2006. Fine structure of the compound eye of the fungus beetle *Neotriplax lewisi* (Coleoptera, Cucujiformia, Erotylidae). Invertebrate Biology 125: 265–278.

Mora AADR. 2014. A preliminary comparative study on structure and main characteristics of compound eyes in four Mexican cone borers *Conophthorus* spp (Coleoptera: Scolytinae). Arthropods 3: 147–160.

Nilsson DE. 1989. Optics and evolution of the compound eye, pp. 30–73 *In* Stavenga DG, Hardie RC [eds.], Facets of Vision. Springer, Berlin.

Nordstrom P, Warrant EJ. 2000. Temperature-induced pupil movements in insect superposition eyes. Journal of Experimental Biology 203: 685–692.

Shaw SR. 1978. The extracellular space and blood-eye barrier in an insect retina: an ultrastructural study. Cell and Tissue Research 188: 35–61.

Smola U, Tscharntke H. 1979. Twisted rhabdomeres in the dipteran eye. Journal of Comparative Physiology 133: 291–297.

Snyder AW. 1973. Polarization sensitivity of individual retinula cells. Journal of Comparative Physiology 83: 331–360.

Somanathan H, Kelber A, Borges RM,Wallén R, Warrant EJ. 2009. Visual ecology of Indian carpenter bees II: adaptations of eyes and ocelli to nocturnal and diurnal lifestyles. Journal of Comparative Physiology A 195: 571–583.

Stark SW, Ivanyshyn AM, Hu KG. 1976. Spectral sensitivities and photopigments in adaptation of fly visual receptors. Naturwissenschaften 63: 513–518.

Stavenga DG. 2003. Angular and spectral sensitivity of fly photoreceptors. II. Dependence on facet lens F-number and rhabdomere type in *Drosophila*. Journal of Comparative Physiology A 189: 189–202.

Vidyasagar PSPV, Keshava-Bhat S. 1991. Pest management in coconut gardens. Journal of Plant Crops 19: 163–182.

Wachmann E. 1977. A comparative analysis of the ultrastructural organization in the eyes of *Cucujiformia* (Insecta, Coleoptera) with particular attention to the *Chrysomelidae*. Zoomorphologie 88: 95–131.

Wachmann E. 1979. Comparative morphological investigations on the ultrastructure of long-horned beetles (Coleoptera, Cerambycidae). Zoomorphologie 92: 19–48.

Warrant EJ. 1999. Seeing better at night: life style, eye design and the optimum strategy of spatial and temporal summation. Vision Research 39: 1611–1630.